Energy-Efficient Directional Charging Strategy for Wireless Rechargeable Sensor Networks

Donghyun Lee, Cheol Lee, Gunhee Jang, Woongsoo Na, and Sungrae Cho

***Abstract*—Mobile chargers (MCs) equipped with radio frequency (RF)-based wireless power transfer (WPT) modules have been suggested as a possible solution to battery constraints in wireless rechargeable sensor networks (WRSNs). In RF-based WPT, charging efficiency decreases significantly as the charging distance increases. Therefore, single-charging consumes less energy than multicharging because it can generally charge a sensor node at a closer range. However, when the density of nodes is high, multicharging may achieve higher efficiency. We propose an energy-efficient adaptive directional charging (EEADC) algorithm that considers the density of sensor nodes to adaptively choose single- or multicharging. The EEADC exploits directional antennas to concentrate the energy and improve energy efficiency and identifies the optimum charging points and beam directions to minimize energy consumption. In the EEADC, clustering is performed by considering the density of the sensor nodes. After clustering, the clusters are classified into single-charging/multicharging clusters according to the number of sensor nodes in each cluster. Next, the charging strategy is determined according to the type of cluster. In the case of a multicharging cluster, the problem is nonconvex. Therefore, a discretized charging strategy decision (DCSD) algorithm is proposed. The performance evaluation indicates that EEADC outperforms two existing methods in terms of power consumption and charging delay by 10% and 9%, respectively.**

***Index Terms*—Wireless power transfer, wireless rechargeable sensor networks, mobile charger, directional wireless power transfer**

I. Introduction

RECENTLY, the use of wireless rechargeable sensor networks (WRSNs) has increased in many fields, such as smart factories [1], smart vehicles, and smart cities. The location of the wireless sensor network (WSN) does not need to be optimized or determined in advance [2]. This allows for the random placement of rechargeable sensors in inaccessible terrain or disaster situations. Applications include military and environmental purposes. By dropping sensor nodes in large quantities from airplanes, sensor networks can be quickly deployed to configure networks such as communication, surveillance, reconnaissance, and targeting systems [3]. In addition, sensors can be deployed in inaccessible areas that are biologically or chemically contaminated to provide remote assistance. However, battery-powered WRSNs often hamper the smooth functioning of networks because of their limited energy. Moreover, access to conflict zones or contaminated environments is limited. To resolve this limitation, research is being conducted on mobile chargers (MCs) based on vehicles equipped with a wireless power transfer (WPT) module that travel to areas where sensor nodes are arranged to charge sensor batteries.

In particular, owing to the higher energy efficiency, research employing directional antennas in WPT modules is being conducted to concentrate transmitted energy onto nodes. In [4], clustering was performed: an MC charged a cluster head, which then transferred its energy to its uncharged nodes. This method resulted in some energy loss owing to the distances among nodes. In particular, [4] proposed a *single-charging* method in which the MC charges one sensor at a time. In [5], an omnidirectional antenna was used for multicharging. However, because the omnidirectional antenna transmitted power in all directions, some energy was wasted. In [6], a WRSN was charged using a directional antenna via a multi-charging method. It determines charging points (or *anchors*) from candidate charging points by considering the energy consumption of the MC. The implementation in [7] was tested in [6]. Unlike [6], [7] minimized the charging delay at the given anchors.

However, multicharging is not always the best option. It may lead to a lower power transfer efficiency if the sensors are located far from the MC, even if they are densely deployed. Therefore, the charging method (i.e., single or multicharging) should be chosen adaptively based on the current topology of the sensors. In this study, we propose a mobile charging strategy, referred to as the energy-efficient adaptive directional charging (EEADC) algorithm, which determines whether to use the single-charging or multicharging method according to the node density. Unlike [6], [7], EEADC determines the optimum charging points, beam directions, charging power, and charging time by considering the node density to minimize the overall energy consumption. EEADC consists of two stages. In the first stage, clustering is performed by considering the density of sensor nodes using the well-known mean-shift algorithm [8]. After clustering, each cluster is classified as a single-charging or multicharging cluster according to the

This research was supported in part by the Chung-Ang University Research Scholarship Grants in 2020 and in part by Basic Science Research Program through the National Research Foundation of Korea(NRF) funded by the Ministry of Education(2019R1A6A1A03032988).

D. Lee, and S. Cho are with the School of Computer Science and Engineering, Chung-Ang University, Seoul 06974, South Korea. (e-mail: dhlee@uclab.re.kr; srcho@cau.ac.kr)

C. Lee is with the Naver Corporation, Seongnam 13561, South Korea. (e-mail: clee@uclab.re.kr)

G. Jang is with Qucell Networks, Seongnam 13590, South Korea. (e-mail: ghjang@uclab.re.kr)

W. Na is with the Department of Computer Science and Engineering, Kongju National University, Cheonan 31080, South Korea (e-mail: wsna@kongju.ac.kr)

Sungrae Cho is the corresponding author for this paper

number of sensor nodes it contains. The charging strategy (single-charging/multicharging), which includes the charging point, beam direction, charging power, and charging time, is then determined according to the type of cluster. In the second stage, if a cluster is classified as a multicharging cluster, the problem of determining the charging strategy is nonconvex. Thus, in this study, an efficient discretized charging strategy decision (DCSD) algorithm is proposed. The DCSD divides the problem into two subproblems, and candidate charging points are obtained by solving the first subproblem. In the second subproblem, the point with the lowest energy consumption among the candidate charging points is selected as the optimal charging point.

This study provides the following main contributions.

- To the best of our knowledge, the EEADC algorithm is the first attempt to consider single-charging/multicharging strategies adaptively. In our work, because the charging strategy is dynamically determined according to the charging efficiency, we can always achieve the same charging efficiency or better than single charging, and reduce energy waste due to overuse of multicharging.
- Instead of using the K-means algorithm, which is employed in the majority of MC clustering methods, EEADC exploits a mean-shift algorithm considering node density to determine single/multicharging clusters.
- In the case of a multicharging cluster, because the problem of finding the optimal charging point, beam direction, charging power, and charging time is a nonconvex problem, the DCSD algorithm is proposed to solve the problem efficiently.

The remainder of this paper is organized as follows. In Section II, we present a literature review of charging strategies for wireless rechargeable sensor networks. Section III introduces the basic charging and network models, basic assumptions, and the adaptive charging scheduling problem. Section IV describes EEADC and DCSD. Section V presents the simulation results of EEADC in terms of energy consumption and charging delay. The conclusions are presented in Section VI.

II. Related Work

The most important issue regarding WRSNs is the efficient use of the limited energy available to maintain the network [9]. Wireless power transmission and MCs have been introduced to overcome this limitation. In this regard, many related studies, including this study, have focused on various efficiencies. To the best of our knowledge, Wang *et al.* proposed the first technique to use a fixed charger with directional antennas [10]. They proposed a radio frequency (RF)-based WPT in which a base station (BS) with multiple directional antennas charged the sensor nodes. In [11], a fixed charger employing a directional antenna was presented, wherein the charger placement was optimized using a charging utility algorithm. Zhihua *et al.* [12] proposed the use of *mobile* directional chargers to charge WRSNs. The charging area formed a grid based on the directions of the antennas. However, the grid was optimized without considering energy consumption. In contrast, a charging method that charges multiple nodes simultaneously referred to as the *multicharging* method was proposed in [10]–[12]. In [13], the authors attempted to solve the energy problem in WRSNs that provide mobile multimedia services. In these WRSNs, nodes far away from other nodes always use a higher amount of energy to transmit data. As a result, there is a high probability that the available residual energy will be low. In [13], the authors attempted to balance the energy among the nodes of WRSNs through appropriate routing and charging algorithms and proposed a method for obtaining a fast convergence value using an efficient algorithm. In [14], the authors attempted to charge the nodes of large-scale WRSNs using a multihop method. However, the single-charging problem approach resulted in poor scalability regarding large-scale WRSNs. In [14], clustering was performed, and the nodes were charged using a multihop method. The goal was to minimize the number of nodes that became inoperable because of battery exhaustion. In [15], the goal was to maximize the charge compensation during the MC's visits to the WRSNs. The scheduling problem for the MC, presented in [15], was NP-hard, and an approximation algorithm was proposed. Various approximation ratios were set, and the calculation speed was determined accordingly. The authors in [16] presented a multicharging method. The charging utility was defined to minimize the expiration time of the WRSN nodes, and aimed to maximize the WRSN's utility. In addition, the energy consumption of the MC was minimized by minimizing the length of the charging tour. To achieve this, an approximation algorithm was first proposed to solve the problem without considering the energy limitations of the MC. An efficient heuristic algorithm that considers the energy constraints of the MC was also proposed.

Yanjun *et al.* [17] aimed to charge the batteries of wearable devices remotely. In this study, an MC was not involved; a fixed charger was used, and the aim was to deploy the charger efficiently by minimizing the distance between the charger and any wearable devices to ensure that the energy of the devices was not exhausted. This study proved that the proposed problem was NP-complete, and a greedy-heuristic algorithm and an approximation algorithm were proposed to solve the problem. The authors in [18] considered the Mine Internet of Things in two dimensions. Several MCs were used in this study in combination with a distributed cooperative algorithm to solve the problem effectively in this situation. The distributed cooperative algorithm divided the roadway into several sections, and each MC was responsible for one section. The algorithm was verified through various simulations according to the length of the sections and the case in which an MC battery constraint existed. In [19], WRSNs were charged through a hybrid-mode–based model named MERSH. The WRSNs were maintained by combining the advantages of existing online and offline scheduling methods. In MERSH, the nodes can send a charge request to the MC when the residual energy falls below a certain level. The route is optimized whenever a request arrives. When the energy of the nodes changes to high dynamics, MERSH dynamically adjusts the charging time of each node.

In [20], scheduling was optimized by considering multiple MCs at the same time. First, the study aimed to minimize the

energy consumption of the MCs while guaranteeing that the energy of all sensors was not exhausted. This problem was represented by mixed-integer linear programming. Second, the problem was solved by reducing the computation time using the decomposition method. The problem was divided in two—MC moving time and charging time—and repeatedly solved. In [21], the number of MCs was minimized when considering multiple MCs. First, the study aimed to ensure that all sensors did not run out of battery power. Second, each MC minimized the use of its remaining energy at the end of each visit. To solve this problem effectively, an algorithm based on the fairness of all sensors was proposed. The algorithm was verified through simulations based on the length of the sections, number of sensors, and number of chargers.

In [22] and [23], several MC scheduling problems were addressed. In [22], the sensor nodes were charged only when their energy fell below a certain level. Each node had a specified charging time window and was charged within that window. Moreover, in a large-scale network, using a single MC to charge all nodes was difficult; therefore, multiple MCs were used. In the study, the problems were solved using genetic algorithms. In [24], several MCs moved to various charge sensor nodes. Unlike other studies, the MC movement paths were fixed, and adjustments were made to MC speed. This study aimed to minimize the time required to complete charging. The problem was defined using an approximation strategy that divided each path into discretized segments. By converting the problem to Lagrangian duals, an efficient distributed algorithm was proposed.

In the aforementioned schemes, the MC does not consider the density of the sensor nodes. Only single-charging or multicharging is considered. If charging is performed considering the density of the sensor nodes, the energy consumption can be further reduced. Therefore, the scheme proposed in this study adaptively considers the density.

III. Adaptive Directional Charging Scheduling Problem

We consider a WRSN where sensor nodes are fixed in a factory or terrain that sense the surrounding environment [25], [26]. In [1], the sensor nodes were driven by energy harvesting and were built for real-time condition monitoring of high-power equipment in a factory. However, it is inefficient to install an energy-harvesting device for each sensor in a large-scale WSN, and because energy harvesting is sensitive to the environment, providing a stable energy supply is impossible. This problem can be solved by utilizing a wireless mobile charger (WMC), which can periodically provide stable power. Therefore, we propose EEADC for efficiently charging sensor nodes through a WMC using a directional antenna. EEADC 1) analyzes the topology of the network and then determines whether single-charge or multicharge conditions apply according to the charging efficiency, 2) in the case of multiple charging, the optimum charging point is determined using the proposed DCSD algorithm, and 3) the WMC moves along the Hamiltonian cycle and charges the sensor nodes.

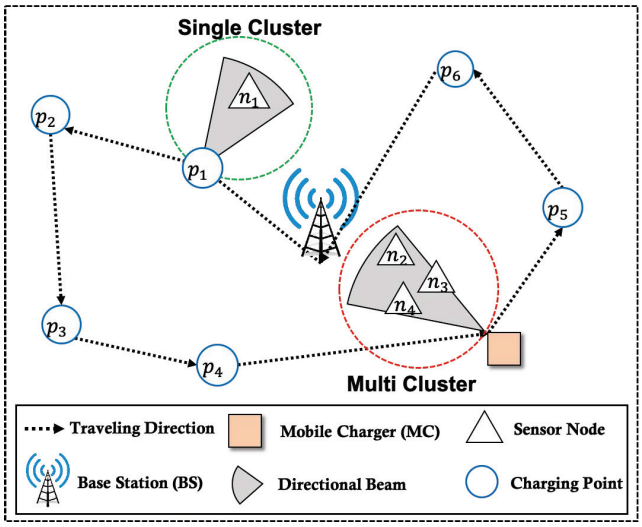

Fig. 1. Overall network model.

In this section, we investigate an adaptive directional charging scheduling (ADCS) problem. The notations used in this study are listed in Table I.

A. Charging Model

In this study, we employ an RF-based WPT, which transmits power according to the following Friis model [27]:

$$P^R = \frac{G^T G^R \gamma}{L_p} \left(\frac{\lambda}{4\pi (D+\beta)} \right)^{\alpha} P^T, \tag{1}$$

where P^R, G^T, and G^R are the received power, transmitted antenna gain, and received antenna gain, respectively. Furthermore, L_p is the polarization loss, γ is the efficiency of the rectifier in the receiver module, λ is the RF wavelength, β is a parameter used to adjust the Friis free-space equation for short-distance transmission, α is the path-loss coefficient, D is the distance between the transmitter and the receiver, and P^T is the transmitted power.

Fig. 1 shows the network model for the proposed system. The sensor nodes are assumed to be deployed in a two-dimensional (2D) field. Each sensor node, n_i, sends a charging request $\text{REQ}_i = \{B_i, B_{\text{max}}, n_i, x_i, y_i\}$ to the BS when the charge level in its battery is lower than the threshold B_{th}. B_i and B_{max} are the current battery level of the i-th node and its maximum battery capacity of the sensor node, respectively. x_i and y_i denote the position of the ith node. The set of nodes is given by $\mathbb{N} = \{n_1, n_2, n_3, ..., n_N\}$, where N is the total number of nodes in the network. Upon receiving the charging requests, the BS schedules the charging strategy and path of the MC based on the ADCS results. The MC then travels from the BS along the determined path to charge the sensor(s) at each charging point (p_i) in the network. According to the scheduling result, the MC adaptively employs the single-charging method, wherein it directly visits and charges a single node (*single-charging cluster*), or the multicharging method, wherein it visits the appropriate charging point to charge multiple nodes simultaneously (*multicharging cluster*).

B. Energy Consumption Model

In this study, each sensor node generates data and transmits the data to the BS in the center of the network. It is assumed that battery-aware multihop routing is applied to transmit the sensor data to the BS. Each sensor node expends most of its available energy when sending and receiving data. Therefore, we adopt the following battery-aware multihop energy consumption model [5]:

$$e_i = \sigma \sum_{l \in \mathbb{N}}^{l \neq i} f_l^i + \sum_{m \in \mathbb{N}}^{m \neq i} C_i^m \cdot f_i^m + C_i^{BS} \cdot f_i^{BS}, \tag{2}$$

where e_i is the energy consumption rate of node i, σ represents the energy consumption rate for receiving one data unit, and f_i^l is the data flow rate from sensor l to sensor i. $\sum_{m \in \mathbb{N}}^{m \neq i} C_i^m \cdot f_i^m + C_i^{BS} \cdot f_i^{BS}$ is the energy required for transmission, where C_i^m and C_i^{BS} represent the energy consumption rate for transmitting one data unit from node i to sensor node m and to the BS, respectively. f_i^m and f_i^{BS} are the transmit flow rates from sensor i to sensor m and BS, respectively. The sensor nodes use the multihop routing protocol when their battery level is lower than that of the neighboring sensor nodes, whereas the one-hop routing protocol is used to send data directly to the BS when the battery level is higher than that of neighboring sensor nodes [28]. The energy consumption rate of the sensor nodes is assumed constant.

C. Directional Charging Scheduling Problem

In our model, we assume that the charging efficiency increases linearly as the number of nodes increases. In [27], the relative gap between the sum of the individual charging power and the simultaneous charging power was demonstrated to be small. Moreover, the charging efficiency of RF-based charging technology is extremely low (if the distance between the sensor node and the charging point is greater than 20 cm, the RF-charging efficiency is 1% [29]), whereas as the number of nodes increases, the charging efficiency increases linearly [30]. Therefore, the objective function is expressed in a relaxed form without constraints as follows. We first define the adaptive directional charging scheduling problem as follows:

$$\min \ E_{\text{total}}(\mathbb{P}) = E_M(\mathbb{P}) + \sum_{p_i \in \mathbb{P}} E_C(p_i), \tag{3}$$

where $\mathbb{P} = \{p_1, p_2, ..., p_P\}$ represents a set of charging points available to the MC, P is the number of charging points, $E_M(\mathbb{P})$ represents the quantity of energy consumed to move the MC when the selected charging points $(p_1, p_2, ...p_P)$ are visited, and $E_C(p_i)$ represents the energy consumption of the i-th point to be charged.

Furthermore, we make the following assumptions.

- Similar to [6], the MC battery capacity is large enough to charge all nodes on the network without interruption.
- The carrier frequency of the transmit RF signal is 900 MHz, and the receiving antenna gain of the sensor is $G^R = 1$ dBi.

TABLE I
SYMBOLS AND DEFINITIONS

Symbol	Definition
P^T	Transmitted power
P^R	Received power
G^T	Transmitted antenna gain
G^R	Received antenna gain
γ	Efficiency of rectifier in receive module
L_p	Polarization loss
λ	RF wavelength
D	Distance between transmitter and receiver
α	Path-loss coefficient
β	Adjustment parameter for short-distance transmission
$\mathbb{N}$	Set of sensor nodes
n_i	Each sensor node
N	Number of sensor nodes
x_i, y_i	Coordinates of sensor node n_i
B_i	Residual battery level of sensor node n_i
B_{max}	Battery capacity of normal sensor node
$B_{\text{max}}^{\text{adv}}$	Battery capacity of advanced sensor node
REQ_i	Charging request by sensor node n_i
$\mathbb{P}$	Set of charging points
p_i	Each charging point
P	Number of charging points
R	Maximum cluster radius
$\mathbb{C}$	Set of clusters
$\mathbb{C}_j$	Each cluster
cx_j, cy_j	Coordinates of charging point for $\mathbb{C}_j$
$\vec{d_j}$	Directional beam vector at $\mathbb{C}_j$
u_j, v_j	Element of directional beam vector at $\vec{d_j}$
θ	Beamwidth angle
T_j	Charging time at $\mathbb{C}_j$
P_{ij}^R	Power received by n_i from $\mathbb{C}_j$
P_j^T	Transmitted power at $\mathbb{C}_j$

- After the MC arrives at a charging point, it completely charges all neighboring sensor nodes and moves to the next charging point.
- To better focus on the problem proposed in this study, the directional beam of the MC is assumed to be uniformly sectored [6], [10].
- The charging efficiency increases with the number of receiving nodes, and the objective function is expressed in a relaxed form without constraints.
- To better focus on the problem proposed in this study, we assume that there are no obstacles in the path of the mobile charger [5], [25].

IV. Energy-Efficient Adaptive Directional Charging (EEADC) Algorithm

To solve the adaptive charging scheduling problem in III, we propose an energy-efficient adaptive directional charging (EEADC) algorithm. The EEADC consists of the following procedures:

1) Clustering of sensor nodes in the given topology (without determining charging points, only grouping),
2) Determining the charging strategy, which includes charging type (*single-charging/multicharging*), charging point, beam direction, charging power, and charging time,
3) Path selection for the MC along the charging points.

In Fig. 2, in the first step, BS analyzes the topology by collecting location information and status information from

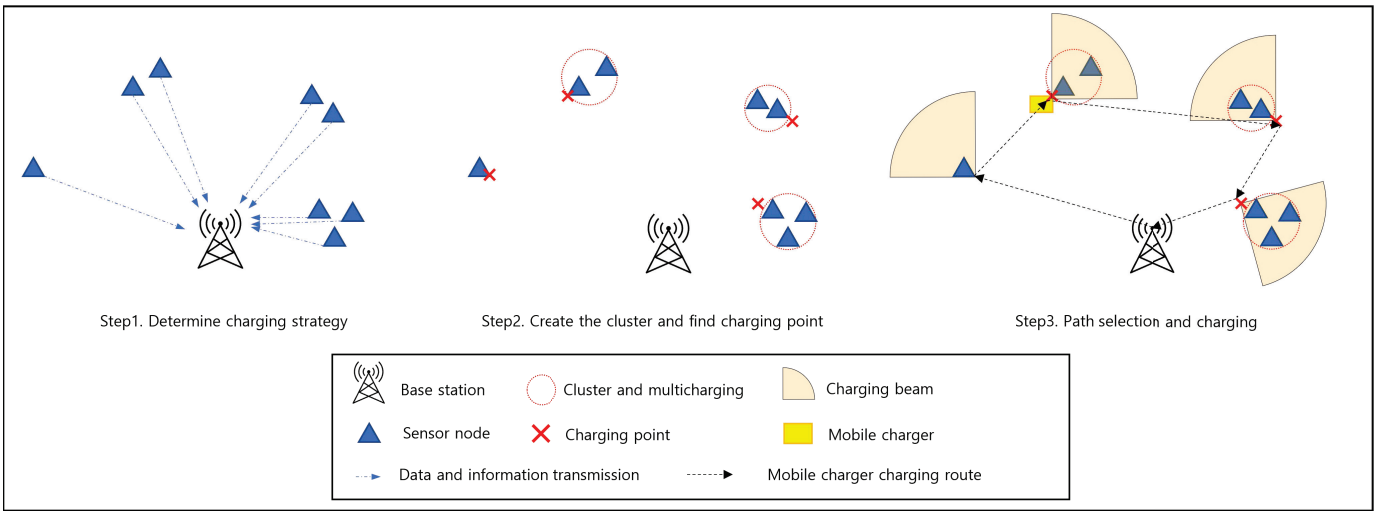

Fig. 2. Three-step procedures of EEADC algorithm

sensor nodes. In the second step, find charging points, charging beam directions and charging time considering the remaining battery level of each node in the cluster. Finally, the charging path is determined.

A. Mean-shift based Clustering

First, EEADC forms clusters based on the density of the sensor nodes. EEADC adopts a mean-shift clustering algorithm [8], as indicated in Algorithm 1. The mean-shift algorithm is an algorithm that repeats until convergence of the process of determining the coordinate average value of nodes within an effective radius R from the center of the cluster is reached. Therefore, the mean-shift algorithm automatically determines the appropriate number of clusters and there is no need to calculate the number of clusters. According to Algorithm 1, the EEADC selects a candidate cluster head p[1] randomly from the available sensor nodes, and it is treated as the center of the cluster (line 5). Then, the drift mean point (average coordinate point) p_{mean} of the sensor nodes within R from the previous cluster center point, p, is computed (line 8). Next, a new cluster center is created by updating p by p_{mean} (line 9). If the updated p is the same as the previous p, that is, p has converged (lines 6–13), a cluster is created that contains all nodes within the range R from p (lines 14–16). This process is repeated until the set $\mathbb{N}$ of the sensor nodes is empty. In this step, the cluster centers are not charging points; they are used only for grouping the sensor nodes.

The K-means clustering algorithm can be utilized for our model. However, it cannot directly control the node densities of the clusters. Instead, the mean-shift algorithm is considered in our model because the node density of clusters can be adjusted immediately through R. Therefore, the mean-shift algorithm has a higher likelihood of producing multicharging clusters to achieve better energy efficiency.

[1] p is not necessarily a sensor node.

Algorithm 1 Mean-shift clustering algorithm

1: **Input**: Set of sensor nodes $\mathbb{N}$, cluster radius R
2: $j = 1$ // Cluster index
3: **while** $\mathbb{N} \neq \emptyset$ **do**
4: Convergence = *false*
5: Select initial point $p \in \mathbb{N}$
6: **while** Convergence = *false* **do**
7: $p_{\text{pre}} \leftarrow p$
8: Calculate drift mean point p_{mean} of the sensor nodes within R from p.
9: $p \leftarrow p_{\text{mean}}$
10: **if** $p = p_{\text{pre}}$ **then**
11: Convergence = *true*;
12: **end if**
13: **end while**
14: $\mathbb{C}_j \leftarrow$ All sensor nodes within range R from p.
15: $\mathbb{C} = \mathbb{C} \bigcup \mathbb{C}_j$
16: $\mathbb{N} = \mathbb{N} - \mathbb{C}_j$
17: $j = j + 1$
18: **end while**
19: **return** cluster set $\mathbb{C}$

B. Determining the charging strategy

After clustering, it is necessary to determine the charging strategy, which includes charging type (*single-charging/multicharging*), charging point, beam direction, charging power, and charging time. The charging strategy is assigned depending on the following conditions.

1) In the case of a single-charging cluster with only one sensor node, the node is charged through the single-charging method. In this case, the charging point approximately becomes the location of the single sensor node and is expressed as follows:

$$p_j = (cx_j, cy_j) \approx (x_i, y_i),\ n_i \in \mathbb{C}_j, \tag{4}$$

where cx_j and cy_j are the x, y coordinates of the charging point of the jth cluster, p_j.

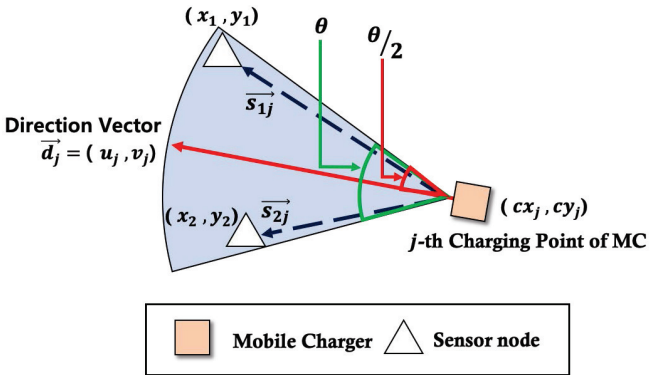

Fig. 3. Charging point, beam direction, charging power, and charging time in the multicharging case.

2) In the case of multicharging clusters, we should minimize the energy consumption and charging time of the MC at each charging point as follows:

$$\textbf{(P1)} \ \min \ P_j^T \cdot T_j, \tag{5}$$

where P_j^T and T_j are the transmitted power of the MC and the charging time in the j-th cluster, respectively. Charging times for all clusters, T_j, must be greater than 0.

$$T_j \geq 0 \tag{6}$$

As shown in Fig. 3, the directional beam vector of the j-th cluster is $\vec{d_j} = (u_j, v_j)$. Here, θ represents the beamwidth angle. All nodes in the cluster must be within the charging range of the directional beam. To reflect this condition, we introduce an additional vector $\vec{s_{ij}}$, which can be expressed as

$$\vec{s_{ij}} = (x_i - cx_j, \ y_i - cx_j), \ \ \forall n_i \in \mathbb{C}_j, \ \mathbb{C}_j \in \mathbb{C}, \tag{7}$$

where $\vec{s_{ij}}$ represents a vector from the charging points of the j-th cluster to the i-th sensor node, that is, the vector from the charging point to the i-th sensor node in the j-th cluster. Therefore, the following conditions hold:

$$\frac{\vec{d_j} \cdot \vec{s_{ij}}}{\|\vec{d_j}\| \ \|\vec{s_{ij}}\|} \geq \cos\frac{\theta}{2}, \ \ \forall n_i \in \mathbb{C}_j, \ \mathbb{C}_j \in \mathbb{C}, \tag{8}$$

where $\vec{a} \cdot \vec{b}$ is the inner product of $\vec{a}$ and $\vec{b}$, and $\|\vec{d}\|$ is the norm of $\vec{d}$. Condition (8) represents a constraint indicating that the angle between $\vec{d_j}$ and $\vec{s_{ij}}$ should be less than $\theta/2$, which ensures that the i-th sensor node is located within the path of the charging beam irradiating the j-th cluster. Because all nodes in the cluster must be fully charged, the following constraint should be added:

$$P_{ij}^R \cdot T_j \geq B_{\max} - B_i, \ \ \forall n_i \in \mathbb{C}_j, \ \mathbb{C}_j \in \mathbb{C}, \tag{9}$$

where P_{ij}^R represents the power received by the ith node in the j-th cluster. By substituting (1) into (9), we obtain

$$\frac{G^T G^R \gamma}{L_p} \left(\frac{\lambda}{4\pi \left(\text{dist}(i) + \beta\right)} \right)^2 P_j^T \cdot T_j \geq B_{\max} - B_i, \tag{10}$$

where dist(i) is the Euclidean distance between the i-th node and the j-th cluster charging point, which is given by $\sqrt{(x_i - cx_j)^2 + (y_i - cy_j)^2}$. In (10), $G^T, G^R, \gamma, L_p, \lambda, \beta$, and P_j^T are constants similar to those in (1). Thus, these constants can be represented by a single constant ρ.

$$\rho \ = \ \frac{P_j^T G^T G^R \lambda^2 \gamma}{16\pi^2 L_p} \tag{11}$$

Therefore, by substituting ρ and dist(i) into (10), we obtain the following.

$$T_j \cdot \frac{\rho}{(\sqrt{(x_i - cx_j)^2 + (y_i - cy_j)^2} + \beta)^2} \geq B_{\max} - B_i, \tag{12}$$

$$(B_{\max} - B_i) \cdot (\sqrt{(x_i - cx_j)^2 + (y_i - cy_j)^2} + \beta)^2 - T_j \cdot \rho \leq 0. \tag{13}$$

Therefore, if $T_j = 0$, then there is no node remaining in the cluster that requires charging.

Additionally, (8) can be transformed by multiplying by the denominator of the left term as follows.

$$\|\vec{d_j}\| \ \|\vec{s_{ij}}\| \cdot \cos\frac{\theta}{2} - \vec{d_j} \times \vec{s_{ij}} \leq 0, \ \ \forall n_i \in \mathbb{C}_j, \mathbb{C}_j \in \mathbb{C}. \tag{14}$$

To avoid a hazardous condition, the following constraint should be added.

$$P_j^T \leq P_{\max} \tag{15}$$

Then, the optimal solution of the charging point p_j^*, beam direction $\vec{d_j}^*$, charging power P_j^{T*}, and charging time T_j^* for the j-th cluster becomes

$$\textbf{(P1)} \quad (p_j^*, \vec{d_j}^*, P_j^{T*}, T_j^*) = \underset{p_j, \vec{d_j}, P_j^T, T_j}{\arg\min} \ P_j^T \cdot T_j, \tag{16}$$
$$s.t. \ (6), (13), (14), \text{ and } (15)$$

which is derived from (5). However, the Hessian matrices of (13) and (14) are not positive definite, and therefore, **(P1)** is a nonconvex problem. Thus, it can be solved using a subgradient descent method after converting it into a convex form through a **Lagrangian dual function.** In the problem to be solved, the variables to be determined are $p_j, \vec{d_j}, P_j^T$ and T_j. To convert to a Lagrangian dual form, Lagrangian multipliers need to be introduced. In our problem, these are $\boldsymbol{\psi}_j \triangleq \{\psi_{ij}\}$, $\boldsymbol{\mu}_j \triangleq \{\mu_{ij}\}$, $\boldsymbol{\eta}_j \triangleq \{\eta_{ij}\}$, and σ_j. The Lagrangian dual form of problem **(P1)** can then be expressed as follows.

$$\mathcal{L}(p_j, \vec{d_j}, P_j^T, T_j, \boldsymbol{\psi}_j, \boldsymbol{\mu}_j, \boldsymbol{\eta}_j, \sigma_j)$$

$$= P_j^T \cdot T_j + \sigma_j(P_j^T - P_{\max}) - \sum_{n_i \in \mathbb{C}_j} \psi_{ij} \cdot T_j +$$

$$\sum_{n_i \in \mathbb{C}_j} \mu_{ij}\{(B_{\max} - B_i) \cdot (\sqrt{(cx_j - x_i)^2 + (cy_j - y_i)^2} + \beta)^2$$

$$- T_j \cdot \rho\} + \sum_{n_i \in \mathbb{C}_j} \eta_{ij}\{\|\vec{d_j}\| \ \|\vec{s_{ij}}\| \cdot \cos\frac{\theta}{2} - \vec{d_j} \cdot \vec{s_{ij}}\} \tag{17}$$

Lagrangian multipliers must be greater than 0. Thus, the following constraints are added.

$$\boldsymbol{\psi}_j \succcurlyeq 0, \tag{18}$$
$$\boldsymbol{\mu}_j \succcurlyeq 0, \tag{19}$$
$$\boldsymbol{\eta}_j \succcurlyeq 0, \tag{20}$$
$$\sigma_j \geq 0 \tag{21}$$

In the above constraints, $\succcurlyeq$ denotes the componentwise inequality. Then, the Lagrangian dual function of **(P1)** is defined as

$$\textbf{(P2)}\ g(\boldsymbol{\psi}_j, \boldsymbol{\mu}_j, \boldsymbol{\eta}_j, \sigma_j) = \min_{p_j, \vec{d}_j, P_j^T, T_j} \mathcal{L}(p_j, \vec{d}_j, P_j^T, T_j, \boldsymbol{\psi}_j, \boldsymbol{\mu}_j, \boldsymbol{\eta}_j, \sigma_j). \tag{22}$$

The dual problem is to maximize the dual function over the Lagrangian multipliers such that

$$\textbf{(P3)}\ \max_{\boldsymbol{\psi}_j, \boldsymbol{\mu}_j, \boldsymbol{\eta}_j, \sigma_j} g(\boldsymbol{\psi}_j, \boldsymbol{\mu}_j, \boldsymbol{\eta}_j, \sigma_j) \quad s.t.\ (18) - (21). \tag{23}$$

We use the subgradient algorithm to iteratively solve the problem defined by (23). The Lagrangian multipliers are updated iteratively as follows:

$$\psi_{ij}^{w+1} = \left[\psi_{ij}^{w} - T_j \Delta\psi\right]^+, \tag{24}$$

$$\mu_{ij}^{w+1} = [\mu_{ij}^{w} + \{(B_{\max} - B_i) \cdot (\sqrt{(cx_j - x_i)^2 + (cy_j - y_i)^2} + \beta)^2 - T_j \cdot \rho\}\Delta\mu]^+, \tag{25}$$

$$\eta_{ij}^{w+1} = \left[\eta_{ij}^{w} + (\|\vec{d_j}\|\ \|\vec{s_{ij}}\| \cdot \cos\frac{\theta}{2} - \vec{d_j} \cdot \vec{s_{ij}})\Delta\eta\right]^+, \tag{26}$$

$$\sigma_j^{w+1} = \left[\sigma_j^{w} + (P_j^T - P_{\max})\Delta\sigma\right]^+, \tag{27}$$

where $[a]^+ = \max\{a, 0\}$, and $w \in \mathbb{N}_+$ denotes the index of iteration. $\Delta\psi$, $\Delta\mu$, $\Delta\eta$, and $\Delta\sigma$ are small step sizes.

Once we determine the charging point and beam direction after solving **(P1)**, we can easily obtain the charging power P_j^T and charging time T_j. Accordingly, in each iteration, for any given $\boldsymbol{\psi}_j, \boldsymbol{\mu}_j, \boldsymbol{\eta}_j, \sigma_j$, the subproblem **(P2)** can be separated into the following subproblems:

$$\textbf{(P2A)} \min_{p_j, \vec{d_j}} \sum_{n_i \in \mathbb{C}_j} \eta_{ij}\{\|\vec{d_j}\|\ \|\vec{s_{ij}}\| \cdot \cos\frac{\theta}{2} - \vec{d_j} \cdot \vec{s_{ij}}\} + \sum_{n_i \in \mathbb{C}_j} \mu_{ij}\{(B_{\max} - B_i) \cdot (\text{dist}(i) + \beta)^2\} \tag{28}$$

and

$$\textbf{(P2B)} \min_{P_j^T, T_j} (P_j^T \cdot T_j + \sigma_j(P_j^T - P_{\max}) - \sum_{n_i \in \mathbb{C}_j} \psi_{ij} \cdot T_j + \sum_{n_i \in \mathbb{C}_j} \mu_{ij}\{(B_{\max} - B_i) \cdot (\text{dist}(i) + \beta)^2 - T_j \cdot \rho\}. \tag{29}$$

First, it is necessary to solve the **(P2A)** problem to determine the characteristics of the charging point and beam direction. Then, by using the results of **(P2A)**, the charging power and charging time can be calculated by solving the **(P2B)** problem.

However, **(P2A)** is still a nonconvex problem. Therefore, we propose an efficient discretized charging strategy decision (DCSD) algorithm [11], [31] to solve **(P2A)**.

C. Discretized Charging Strategy Decision (DCSD) Algorithm

(P2A) can be restated by *finding the charging point and corresponding beam direction that includes all points tightly and has the minimum sum of the distances from the center to all points.* To this end, the DCSD algorithm (see Fig. 5 is listed in Algorithm 2) and proceeds as follows.

- **Step 1)** Draw the smallest circle containing sensor nodes in the cluster with radius wr_j (lines 2–3). The smallest enclosing circle problem is solved by the Welzl algorithm [32], [33]. We define the center point and the radius of the smallest enclosing circle as (wx_j, wy_j) and wr_j, respectively. In our model, the charging direction of the mobile charger is toward the center of the cluster. Therefore, all sensors should be included in the charging beam, and the location of the edge sensor nodes of the cluster is important when positioning the mobile charger as close to the cluster as possible. Comparing Fig. 4 (a) and Fig. 4 (b), it can be seen that the cluster to which Welzl algorithm is applied can better consider the sensors at the edge of the cluster and locate the charger closer.
- **Step 2)** From the smallest enclosing circle, we must derive fan-shaped circumscribed beams that enclose the smallest enclosing circle (see Fig. 5(b)). These fan-shaped beams can be generated by drawing two lines (blue solid lines) tangent to the smallest enclosing circle, where a constant angle θ exists between the two tangent lines (line 7).
- **Step 3)** If we generate these fan-shaped beams and then connect the centers of the beams, we obtain a circle (the green solid circle in Fig. 5(c)). We can consider the circle as the location of the MC and include it in the solution space for the charging point. However, this solution space is continuous; thus, it is an NP-hard problem. Therefore, to calculate the optimal solution, the DCSD algorithm is used to discretize the solution space.
- **Step 4)** Fig. 5(d) shows the discretized solution space in ϵ-intervals. The discretized solution space is defined as

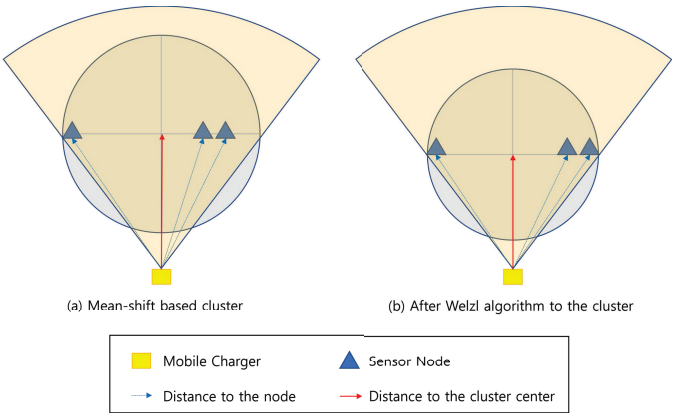

Fig. 4. Smallest enclosing circle using Welzl algorithm

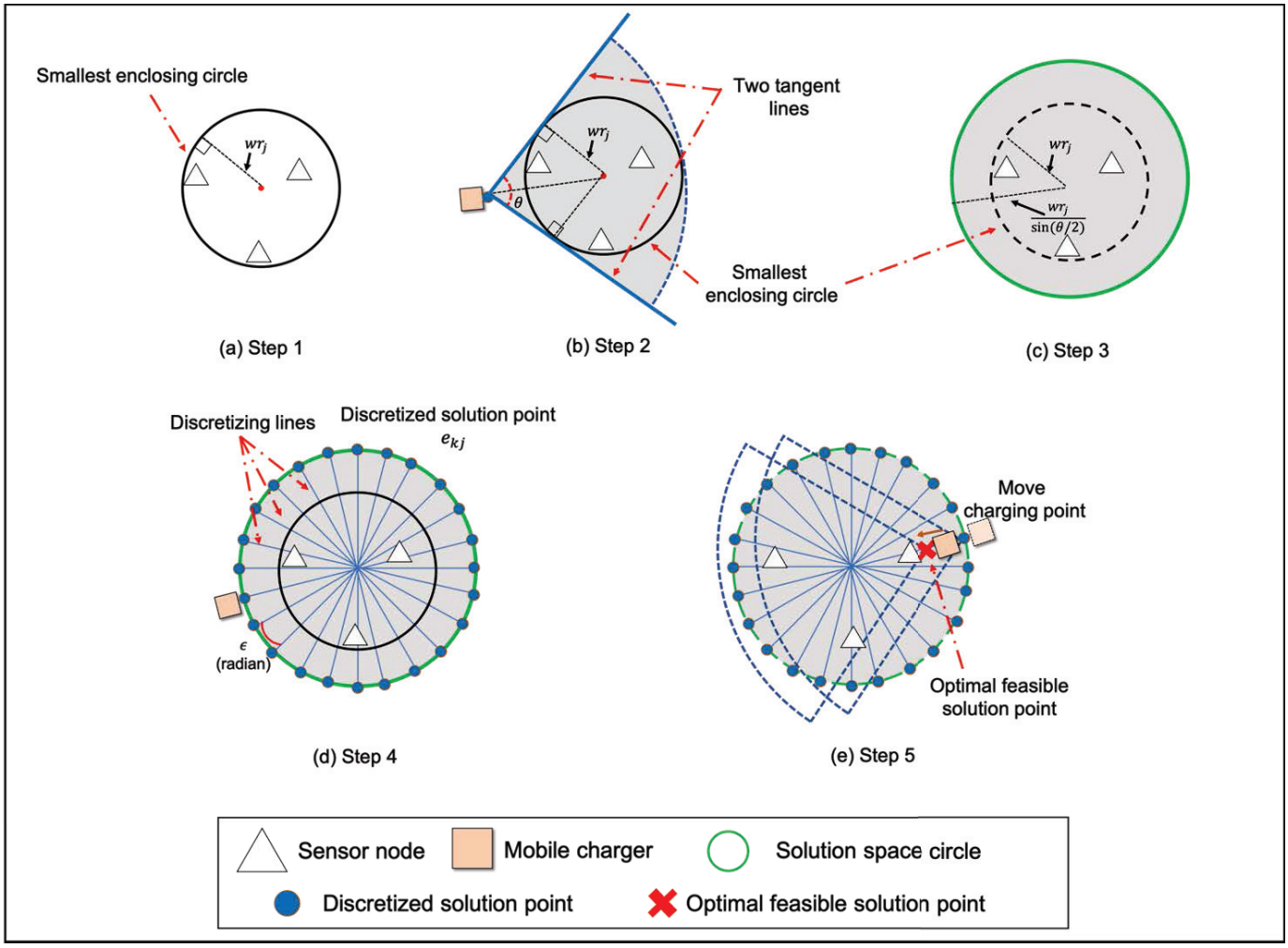

Fig. 5. Discretized charging strategy decision (DCSD) algorithm.

$\mathbb{E}_j$ (line 5). The number of discretized solution points is $\lfloor 2\pi/\epsilon \rfloor$ (line 6). We define the k-th discretized solution point at the j-th cluster as e_{kj} and compute e_{kj} iteratively (lines 6–10).

– **Step 5)** Given the discretized solution points e_{kj}, to solve **(P2A)**, we move each charging point toward the center along the discretized line as much as possible while satisfying (14) (lines 15–17). After moving charging point, **(P2B)** is solved using the determined charging point. In **(P2B)**, $\text{dist}(i) = \sqrt{(cx_j - x_i)^2 + (cy_j - y_i)^2}$. Because the charging point (cx_j, cy_j) and charging power P_j^T are determined, then **(P2B)** can be converted to a linear programming (LP) problem that can easily be solved. Through **(P2B)**, the energy required at each charging point, CE_{kj} can be calculated (line 18). If the calculated CE_{kj} is less than CE_{min}, then the minimum values are updated (lines 19–25).

To solve **(P3)** using the subgradient algorithm, (24)–(27), we repeat the DCSD in each iterative step until the result converges to obtain the final solution.

After determining charging points for every cluster, the order in which the charging points are visited is determined by the shortest distance based on the well-known traveling salesman problem (TSP). In this step, we use a faster heuristic TSP algorithm (LKH-TSP) [5], [34].

D. Time Complexity and Convergence Analysis

Because the EEADC is composed of mean-shift clustering and DCSD, we first analyze the time complexity of the mean-shift algorithm. The mean-shift algorithm repeats until each point converges, and the time complexity of the mean-shift algorithm is known to be $O(N^2)$, where N is the number of sensor nodes in the network [8]. After finding clusters using mean-shift clustering, the DCSD is repeated at every step of the subgradient method. The convex problem **(P3)** can be solved and converted using subgradient-based methods such as the ellipsoid method [24] [35]. From [24], if the number of variables is L, the complexity of the subgradient method based on the number of repeated iterations is $O(L^2)$.

DCSD solves the problem by dividing the circle into ϵ-intervals. Each cluster is divided into $\lfloor \frac{2\pi}{\epsilon} \rfloor$ discretized segments, and for each segment, the e_{kj} satisfying (14) is determined. After determining e_{kj}, we can calculate CE_{kj} from **(P2B)**. Problem **(P2B)** is an LP, so the solution can be obtained within polynomial time. Therefore, by solving **(P2B)**

Algorithm 2 Discretized Charging Strategy Decision (DCSD) Algorithm

Input: Set of sensor nodes in jth cluster $\mathbb{C}_j$, Beamwidth θ
Calculate smallest enclosing circle for $\mathbb{C}_j$ by using Welzl Algorithm
$(wx_j, wy_j), wr_j \leftarrow$ center point and radius of smallest circle, respectively.
$k = 1$, $\epsilon \leftarrow$ discretizing interval
Discretized solution space $\mathbb{E}_j = \emptyset$
for $k \leq \lfloor \frac{2\pi}{\epsilon} \rfloor$ **do**
    Derive fan-shaped circumscribed beams that enclose the smallest enclosing circle.
    $e_{kj} \leftarrow$ center point of k-th fan-shaped beam of j-th cluster.
    $\mathbb{E} = \mathbb{E} \bigcup e_{kj}$
    $k = k + 1$
end for
minimum charging consumed energy CE_{min}
$i = 0$
for $\forall e_{kj} \in \mathbb{E}_j$ **do**
    while Satisfying (14) **do**
        Move e_{kj} toward (wx_j, wy_j)
    end while
    Calculate charging consumed energy CE_{kj} from **(P2B)** with determined charging point e_{kj} and beam direction at that point, $\vec{d}_{kj}$.
    if $i = 0$ **then**
        $\text{CE}_{\text{min}} = \text{CE}_{kj}$, $e_{\text{min}} = e_{kj}$, $\vec{d}_{\text{min}} = \vec{d}_{kj}$
    else
        if $\text{CE}_{kj} \leq \text{CE}_{\text{min}}$ **then**
            $\text{CE}_{\text{min}} = \text{CE}_{kj}$, $e_{\text{min}} = e_{kj}$, $\vec{d}_{\text{min}} = \vec{d}_{kj}$
        end if
    end if
    $i = i + 1$
end for
$(cx_j, cy_j) \leftarrow e_{\text{min}}, \vec{d}_j \leftarrow \vec{d}_{\text{min}}$
return $(cx_j, cy_j), \vec{d}_j, T_j$

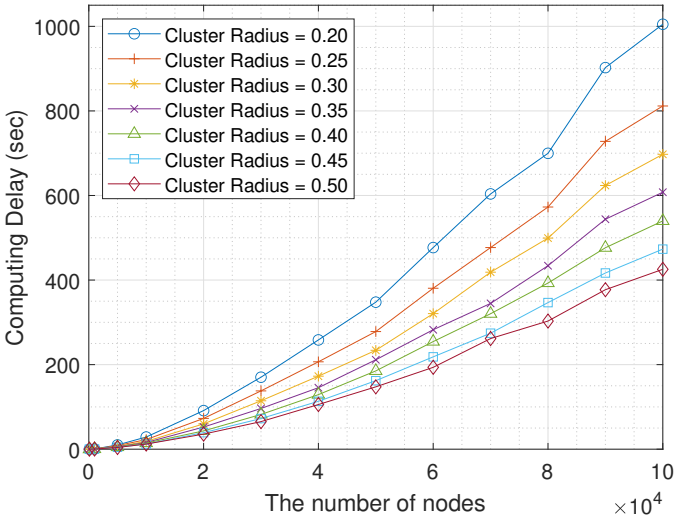

Fig. 6. Computational delay of mean-shift clustering algorithm according to the number of nodes.

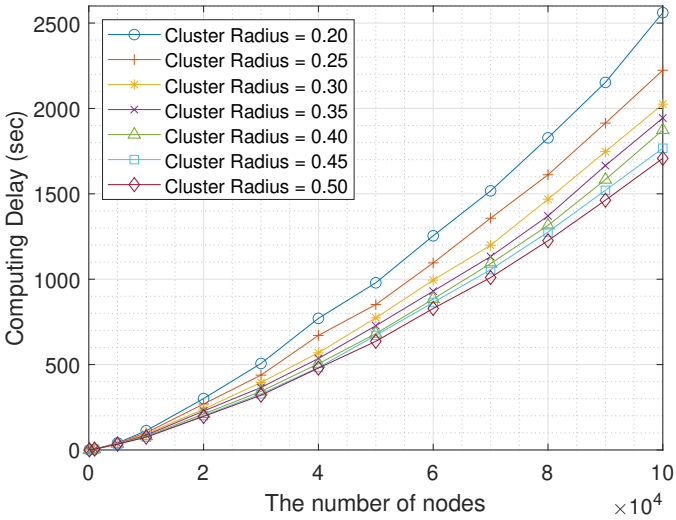

Fig. 7. Computational delay of DCSD algorithm according to the number of nodes.

and assuming that $\lfloor \frac{2\pi}{\epsilon} \rfloor$ is repeated a constant number of times, we can solve the DCSD within polynomial time.

Therefore, if the time to solve LP is assumed to be V, and in the worst case, the number of sensor nodes in one cluster is N, the time complexity for solving **(P3)** is $O(N^2 \cdot V \cdot \lfloor \frac{2\pi}{\epsilon} \rfloor)$. In the case of mean-shift clustering, the time complexity is $O(N^2)$, and in the worst case, N clusters are created. Finally, the total time complexity for convergence is $O(N^2 + V \cdot N^3 \cdot \lfloor \frac{2\pi}{\epsilon} \rfloor)$. The convergence analysis based on the number of nodes for Algorithm1 and Algorithm2 is provided in Fig. 6 and Fig. 7, respectively.

V. Simulation Results

In this section, we analyze the proposed model using simulations. To evaluate the performance of EEADC on various evaluation metrics, we used Python and MATLAB for the simulations. The system used for the simulation is an Intel i7-10700, 16GB RAM. The parallel processing and GPU calculation are not used. The sensor nodes were randomly but uniformly placed using the python rand function on a 2D field. Because the mean-shift algorithm is a clustering technique based on density, it is greatly affected by the distribution of sensor nodes. This is because if the sensor nodes are biased in some places, the efficiency of multicharging comes out abnormally high. Therefore, if the coordinates of the nodes are

TABLE II
Simulation Parameters

Parameters	Values	Parameters	Values
P^T	5 W	G^T	4 dBi
G^R	1 dBi	θ	$\pi/2$
B_{max}	2 J	$B_{\text{max}}^{\text{adv}}$	4 J
λ	0.33 m	v	5 m/s
ϵ	$\pi/90$	L_p	1
γ	1	β	0.3

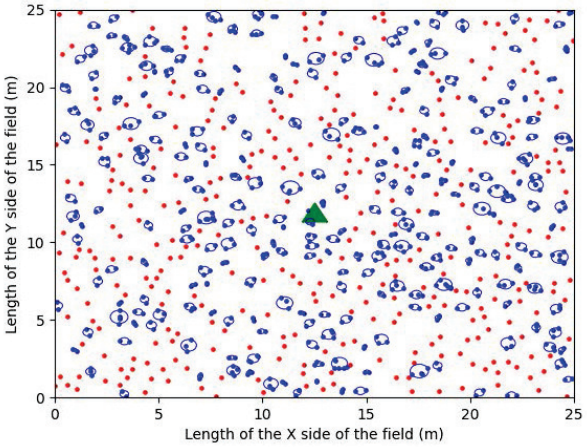

Fig. 8. Network topology.

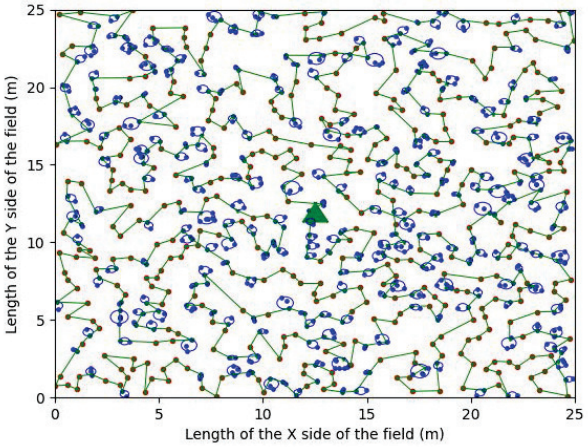

Fig. 9. Generated charging path obtained by applying the LKH-TSP algorithm.

determined using a specific distribution, a biased result may be obtained. To avoid this and to accurately verify the results of the algorithm, all simulations were run 100 times with different random seeds and averaged. During this time, because the charging strategy is determined according to the density of nodes, the experiments were performed by varying the number of nodes between $N = \{500 - 1500\}$, using various network sizes and using various sensor battery capacities. The moving speed of the MC was $v = 5\ m/s$, the energy consumed for the movement was $E_m = 5\ J/m$, the transmit power of the MC was $P_j^T = 5\ W$, the transmit antenna gain of the MC was $G^T = 4$ dBi, and the receiving antenna gain of a node was $G^R = 1$ dBi. The maximum battery capacity of the receiving node was $B_{\max} = 2\ J$, and was randomly initialized from the initial energy range $E_{\text{init}} = [40\%,\ 60\%]$ of the sensor nodes. The number of discretized solution points was 180, i.e., $\epsilon = 2$. In [31], a node direction angle between $-60\,^\circ$ and $60\,^\circ$ in the charging direction was shown to receive significant charging power. Therefore, the charging angle was set from $-45\,^\circ$ to $45\,^\circ$ to ensure a node receives sufficient power in the experiments. In addition, γ, L_p, and β used in (1) were set to 1, 1, and 0.3, respectively, and the RF was set to 900 MHz. Therefore, the RF wavelength was $\lambda = 0.33\ m$.

Fig. 8 shows the system topology with 1000 nodes arranged according to a uniform distribution [36], [37]. In Fig. 8 blue dots within blue circles represent the nodes in multicharging clusters, and red dots represent single-charging nodes. Because we used different random seeds for each simulation, the topology was different each time. Fig. 9 shows the charging path generated by applying the well-known LKH-TSP algorithm [34] in the same network topology. The MC moves along the shortest straight line to each charging point and charges the sensor node(s) [5], [25], [38]. The reason why the charging points are outside the cluster is illustrated in Figure 3.

Fig. 10 shows the energies applicable to our model and the single-charging method according to R for 1000 nodes. If R is 0.1–0.4 (m), our model consumes less energy than the single-charging method. However, when R increases beyond

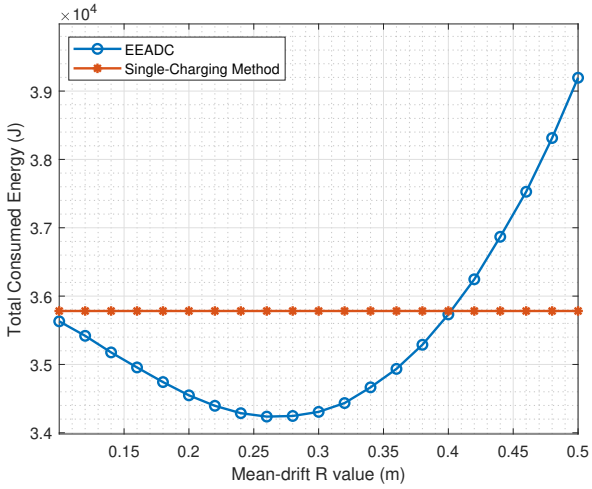

Fig. 10. Comparison of energy consumption of the single-charging method and the proposed model according to the value of R.

0.4 m, the energy consumption rapidly increases because the RF power decreases rapidly with increasing distance. In mean-shift clustering, the R value determines the effective range of the cluster. When using an R value that is too small, almost all nodes are charged using single charging, which is not very different from single-charging all nodes. On the other hand, if R is too large, it must then charge distant nodes. Therefore, the charging efficiency will decrease. Thus, it is necessary to use an appropriate R value. Based on Fig. 10, the R value was set to 0.26 m in the subsequent simulations.

After obtaining the appropriate R value, the mean-shift clustering algorithm is compared with K-means and agglomerative clustering. A density-based clustering algorithm DBSCAN can continue to include nodes in a cluster as long as the nodes are closely listed, allowing the cluster size to grow infinitely. When such a large cluster is created, the distance between the nodes of the cluster and the charging point increases, resulting in lower charging efficiency. Therefore, we exclude DBSCAN.

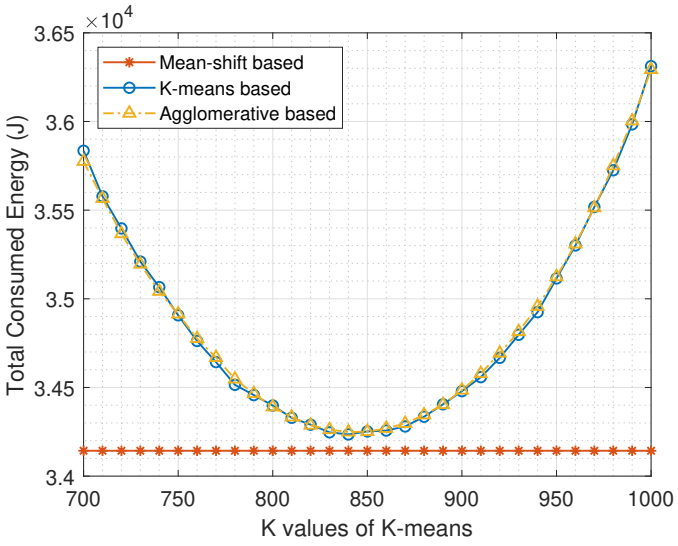

Fig. 11. Comparison of the mean-shift, K-means, and agglomerative algorithms.

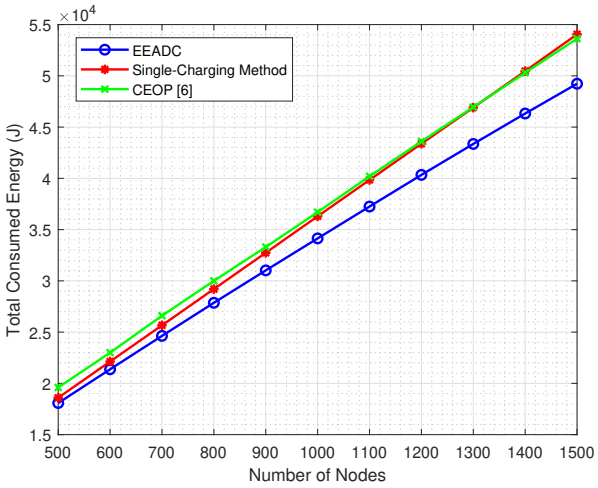

Fig. 12. Single-charging method, proposed EEADC, and CEOP [6] are compared regarding energy consumption versus number of nodes.

Fig. 11 shows the differences among these methods. In Section IV-A, we performed clustering using the mean-shift algorithm in EEADC because it is difficult for agglomerative and K-means to determine an appropriate number of clusters. In addition, even if a specific number of clusters is determined, the result may be significantly different if the node deployment is changed, because the value obtained does not consider the topology of the sensor nodes.

To compare the three clustering methods, first, a simulation was performed using mean-shift clustering and the number of specified clusters was calculated. Subsequently, the other two algorithms were tested in the same range. In Fig. 11, the number of clusters determined through the mean-shift algorithm was 850. Therefore, simulations were performed by setting the number of clusters in the 700–1000 range.

The simulation results show that the EEADC using the other two clustering algorithms consumes more energy than the mean-shift algorithm. Even if we specify the same number of clusters, there is a considerable difference in performance among the three algorithms. This can be explained by the different approaches taken by the three algorithms. The K-means algorithm determines the grouping of each sensor node based on the nearest cluster head. However, the number of clusters must be specified before clustering. Therefore, this process has greater difficulty considering node density than mean-shift. The agglomerative algorithm is similar to K-means, and the number of clusters must be determined before the node topology is analyzed. A multicharging cluster that considers density increases energy efficiency, but a multicharging cluster that does not properly consider density increases energy consumption because of the energy required to charge any distant nodes. That is, the disadvantages of the K-means and agglomerative algorithms are 1) difficulty in setting an appropriate number of clusters, and 2) they do not consider node density. Therefore, we decided to perform clustering using the mean-shift algorithm in this study.

The scheme proposed in this paper is compared with the single-charging method and the model proposed in [6]. To provide a fair comparison, the spacing of the grid candidate charging points in [6] was set to 0.25 m. Fig. 12 shows the difference in energy consumption as the number of nodes increases. In this simulation, the field size was set to 25 $m \times 25$ m. When the number of nodes is small, multicharging clusters are rarely generated using mean-shift clustering, and there is little difference in the energy consumption between the single-charging method and EEADC. However, as the number of nodes increases, the density of the nodes increases. Therefore, the number of multicharging clusters and the number of sensor nodes in each multicharging cluster increase. As the number of multicharging clusters increases, the energy efficiency of the proposed EEADC increases and the difference in energy consumed between EEADC and the single-charging method increases. In addition, we compare the proposed EEADC with CEOP [6]. CEOP divides the 2D field into grids and sets the vertices of the grids as candidate charging points. In CEOP, among the candidate charging points, the charging points that charge the sensor nodes most efficiently are selected, and a directional beam is determined at each point. CEOP appears to be similar to our scheme. However, CEOP decides the candidate charging points by partitioning the field into a grid (implying that it cannot charge near nodes and your charging points are limited on the grid); thus, it does not take into account the density of sensor nodes. Moreover, the density of sensor nodes is low, so even if charging the nodes one by one, the MC cannot charge near the sensor nodes and the charging points are limited to the grid. As a result, when the density of the sensor nodes is low, multicharging becomes highly inefficient compared to single-charging, and in the end, CEOP consumes more energy in most cases than the single-charging method. However, because CEOP essentially ignores single-charging, it can be regarded as a multicharging method. Therefore, when the density of the sensor nodes increases and the multicharging clusters increase, the energy efficiency increases. In Fig. 12, when the number of sensor nodes is 1300, CEOP consumes slightly less energy than

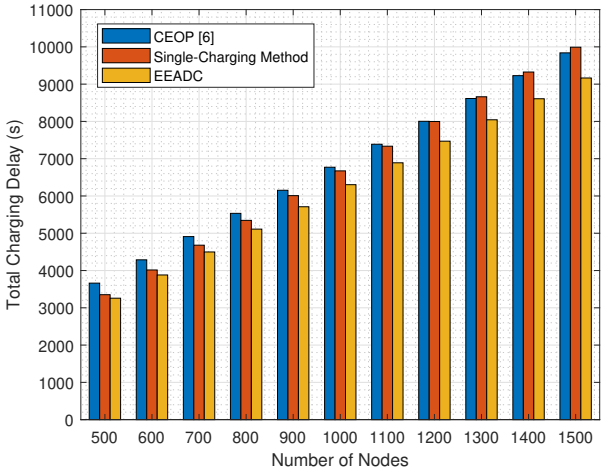

Fig. 13. Single-charging method, proposed EEADC, and CEOP [6] are compared regarding charging delay versus number of nodes.

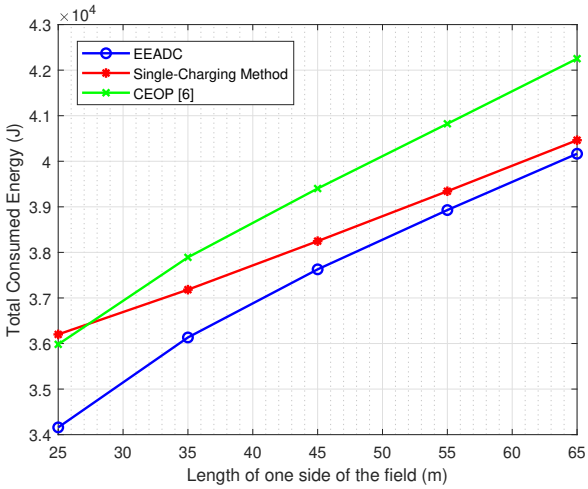

Fig. 14. Single-charging method, proposed EEADC, and CEOP [6] are compared with respect to energy consumption versus field size.

the single-charging method. In conclusion, EEADC, which effectively selects a single-charging or multicharging strategy according to the node density, achieves the best results. When the number of sensor nodes is 1000, EEADC achieves 5.8% better performance than the single-charging method and 7.4% better performance than CEOP. When the number of sensor nodes is 1500, EEADC achieves 9% better performance than the single-charging method and 7.3% better performance than CEOP.

In Fig. 13, we compare the three models in terms of charging delay. The results highlight the difference in the charging delay as the number of nodes increases. The overall result is similar to the result for energy consumption because charging time is proportional to energy consumption. As the number of nodes increases, the difference in the charging delay between the single-charging method and EEADC increases. In addition, the charging delay of CEOP is almost always longer than that of the single-charging method. However, when the number of sensor nodes increases to 1500 nodes, the charging delay of CEOP becomes slightly shorter than that of the single-charging method. The single-charging method performs charging by solving only the TSP problem without analyzing the network topology or the charging efficiency. Accordingly, the computing resources and computation delays required by the BS for calculating the appropriate charging points are not incurred. On the other hand, the proposed EEADC requires these computing resources and the computation delay to analyze the topology even when all sensor nodes are sparsely arranged. Therefore, single-charging can save computing resources in sensor nodes within sparsely deployed systems, whereas EEADC can increase the charging efficiency when densely populated systems are involved.

Fig. 14 shows the change in energy consumption according to the size of the sensor field for a constant number of nodes. As the size of the field increases, energy consumption increases in all three models. First, because only single-charging is always used in the case of the single-charging method, as the size of the field increases, only the moving

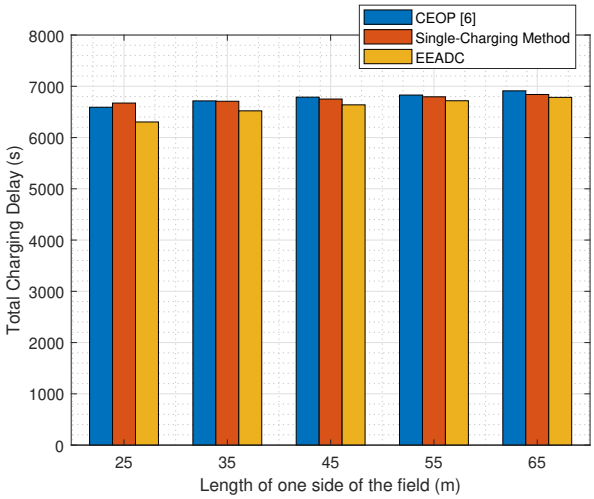

Fig. 15. Single-charging method, proposed EEADC, and CEOP [6] are compared with respect to charging delay versus field size.

distance of the MC increases. When the size of the field is not very large, an increase in the moving distance of the MC does not significantly affect the total energy consumption and a slight improvement compared to the other two methods can be observed. In the case of EEADC, as the size of the field increases, the distance between sensor nodes increases on average, and the number of multicharging clusters generated through mean-shift clustering decreases such that the number of single-charging clusters increases. In other words, its operation is similar to that of the single-charging method. In addition, as the size of the field increases, the moving distance of the MC also increases, as in the single-charging method. Therefore, the increase in energy consumption as the size of the field increases is larger than the single-charging method. However, even when the size of the field increases to 65 m, energy consumption using EEADC is still lower than that of the single-charging method. This is because although the node density has decreased, energy-efficient multicharging

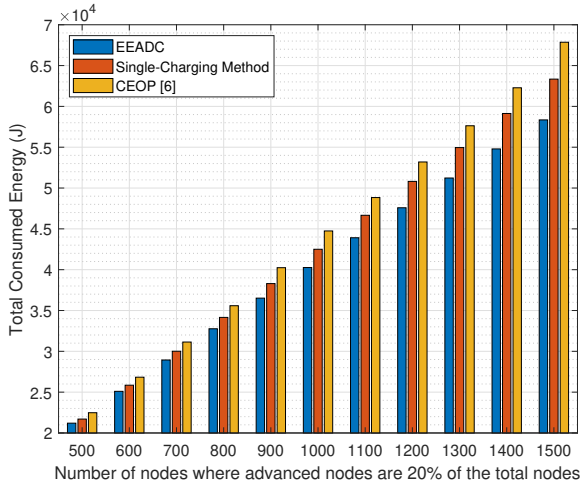

Fig. 16. Single-charging method, proposed EEADC, and CEOP [6] are compared to analyze energy consumption versus number of nodes in a heterogeneous WSN system.

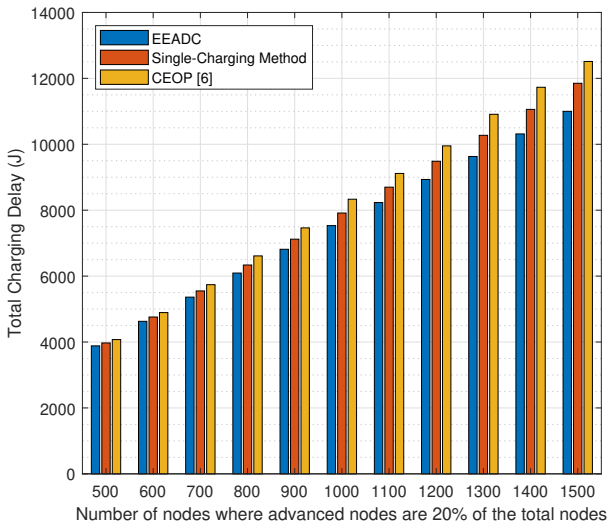

Fig. 17. Single-charging method, proposed EEADC, and CEOP [6] are compared to analyze charging delay versus number of nodes in a heterogeneous WSN system.

clusters are still created. In the case of CEOP, when the field size is 25 m, it achieves better efficiency than single-charging although its energy consumption increases as the size of the field increases. However, CEOP divides the field into grids and selects candidate charging points. Therefore, even if the size of the field increases, the distance between candidate charging points remains constant.

However, because grids are created at fixed intervals without considering node density, the number of sensor nodes in each square grid decreases. As previously observed, the energy efficiency of CEOP increases as the number of sensor nodes in each grid increases. Conversely, if the number of sensor nodes in each grid of the same size decreases, the number of nodes charging at each candidate charging point gradually decreases, and eventually, the case of charging only one node increases (only single-charging clusters are present). However, unlike the single-charging method, because CEOP can be charged only from a vertex in the grid, the MC will be located further from a sensor node. Therefore, energy consumption is greatly increased. As a result, the energy consumption is greater than that of the single-charging method when the field size increases beyond 35 m. Fig. 15 compares the charging delays of the three models according to the size of the field. The results are similar to the results in Fig. 14.

Battery capacity can be different depending on the type of node. Therefore, we add an advanced node type with twice the battery capacity of a normal node to our system model. The number of advanced nodes accounts for 20% of the total system nodes, and the battery capacity is 4 J, which is twice that of normal nodes. We call this type of system a heterogeneous WSN system.

Fig. 16 shows the change in energy consumption as the number of nodes increases. In this simulation, the field size was set to 25 $m \times 25$ m. The maximum battery capacity of the normal receiving node was $B_{\max} = 2$ J, and the advanced node was $B_{\max}^{\text{adv}} = 4$ J and randomly initialized between the initial energy $E_{\text{init}} = [40\%, 60\%]$ of the sensor nodes. When the number of nodes is small, CEOP [6] consumes more energy than the single-charging method because CEOP chooses the charging point to maximize the energy received by the sensor node in the charging beam. However, in a heterogeneous WSN system, an advanced node requires a large amount of energy. Therefore, if there is an advanced node at the edge of the charging beam that is far from the charger, the advanced node needs to be charged at low efficiency even after all other nodes in the charging beam are charged in CEOP. On the other hand, EEADC attempts to find the charging point that requires the least energy to charge a cluster. This creates charging points within the cluster close to the sensor nodes that require the most energy. Therefore, if there are 1500 sensor nodes, EEADC achieves 8.5% better performance than the single-charging method and 16.3% better performance than CEOP. In Fig. 17, we compare the three models in terms of charging delay in a heterogeneous WSN system. The results highlight the difference in the charging delay as the number of nodes increases. The overall result agrees with the previous result. As the number of nodes increases, the difference in the charging delay between the single-charging method and EEADC increases

VI. Conclusion

In this paper, we propose an energy efficient charging method for the sensor nodes in WRSNs, based on an MC employing directional antennas. After mean-drift clustering that considers the density of the nodes in the network, the optimal charging point is determined according to the type of cluster. In particular, in the case of a multicharging cluster, an efficient discretized algorithm is proposed to solve the nonconvex problem. The experimental results show that for most cases, the single-charging method, which charges only one node at a time, minimizes the energy consumed by the MC. However, when the density of the nodes is high,

charging via the multicharging method can reduce the energy consumption.

In [1], WSN was used for real-time monitoring of high-power equipment at a power substation in Kentucky. In [1], 122 sensor nodes were deployed to detect early signs of potential fault conditions in equipment such as transformers and circuit breakers. It can be considered scalable because we considered a sufficiently large WRSN in which up to 1500 sensor nodes are deployed in our work. We expect our model to be useful in larger WRSNs such as power plants, smart factories and even smart cities.

REFERENCES

[1] A. Pal and A. Nasipuri, "Joint power control and routing for rechargeable wireless sensor networks," *IEEE Access*, vol. 7, pp. 123 992–124 007, 2019.

[2] I. Akyildiz, W. Su, Y. Sankarasubramaniam, and E. Cayirci, "Wireless sensor networks: a survey," *Computer Networks*, vol. 38, no. 4, pp. 393–422, 2002.

[3] I. Akyildiz, W. Su, S. Y., and E. Cayirci, "A survey on sensor networks," *IEEE Communications Magazine*, vol. 40, no. 8, pp. 102–114, 2002.

[4] C. Moraes, S. Myung, S. Lee, and D. Har, "Distributed sensor nodes charged by mobile charger with directional antenna and by energy trading for balancing," *Sensors*, vol. 17, no. 1, p. 122, 2017.

[5] W. Na, J. Park, C. Lee, K. Park, J. Kim, and S. Cho, "Energy-efficient mobile charging for wireless power transfer in internet of things networks," *IEEE Internet of Things Journal*, vol. 5, no. 1, pp. 79–92, 2017.

[6] X. Xu, L. Chen, and Z. Cheng, "Optimizing charging efficiency and maintaining sensor network perpetually in mobile directional charging," *Sensors*, vol. 19, no. 12, p. 2657, 2019.

[7] C. Lin, Y. Zhou, F. Ma, J. Deng, L. Wang, and G. Wu, "Minimizing charging delay for directional charging in wireless rechargeable sensor networks," *IEEE INFOCOM 2019 - IEEE Conference on Computer Communications*, pp. 1819–1827, 2019.

[8] Y. Cheng, "Mean shift, mode seeking, and clustering," *IEEE Transactions on Pattern Analysis and Machine Intelligence*, vol. 17, no. 8, pp. 790–799, 1995.

[9] N.-N. Dao, D.-N. Vu, W. Na, J. Kim, and S. Cho, "Sgco: Stabilized green crosshaul orchestration for dense iot offloading services," *IEEE Journal on Selected Areas in Communications*, vol. 36, no. 11, pp. 2538–2548, 2018.

[10] Z. Wang, L. Duan, and R. Zhang, "Adaptively directional wireless power transfer for large-scale sensor networks," *IEEE Journal on Selected Areas in Communications*, vol. 34, no. 5, pp. 1785–1800, 2016.

[11] H. Dai, X. Wang, A. X. Liu, H. Ma, and G. Chen, "Optimizing wireless charger placement for directional charging," *IEEE INFOCOM 2017 - IEEE Conference on Computer Communications*, pp. 1–9, 2017.

[12] Z. Chang, X. Wu, W. Wang, and G. Chen, "Localization in wireless rechargeable sensor networks using mobile directional charger," *2015 IEEE Global Communications Conference (GLOBECOM)*, pp. 1–6, 2015.

[13] F. Liu, H. Lu, T. Wang, and Y. Liu, "An energy-balanced joint routing and charging framework in wireless rechargeable sensor networks for mobile multimedia," *IEEE Access*, vol. 7, pp. 177 637–177 650, 2019.

[14] G. Han, H. Guan, J. Wu, S. Chan, L. Shu, and W. Zhang, "An uneven cluster-based mobile charging algorithm for wireless rechargeable sensor networks," *IEEE Systems Journal*, vol. 13, no. 4, pp. 3747–3758, 2018.

[15] W. Liang, Z. Xu, W. Xu, J. Shi, G. Mao, and S. K. Das, "Approximation algorithms for charging reward maximization in rechargeable sensor networks via a mobile charger," *IEEE/ACM Transactions on Networking*, vol. 25, no. 5, pp. 3161–3174, 2017.

[16] Y. Ma, W. Liang, and W. Xu, "Charging utility maximization in wireless rechargeable sensor networks by charging multiple sensors simultaneously," *IEEE/ACM Transactions on Networking*, vol. 26, no. 4, pp. 1591–1604, 2018.

[17] Y. Li, Y. Chen, C. S. Chen, Z. Wang, and Y.-h. Zhu, "Charging while moving: Deploying wireless chargers for powering wearable devices," *IEEE Transactions on Vehicular Technology*, vol. 67, no. 12, pp. 11 575–11 586, 2018.

[18] Q. Hu, J. Yang, R. Zhang, W. Chen, and B. Li, "Distributed cooperative wireless charging for the mine internet of things," *IEEE Access*, vol. 7, pp. 81 000–81 009, 2019.

[19] Y. Feng, L. Guo, X. Fu, and N. Liu, "Efficient mobile energy replenishment scheme based on hybrid mode for wireless rechargeable sensor networks," *IEEE Sensors Journal*, vol. 19, no. 21, pp. 10 131–10 143, 2019.

[20] L. Mo, A. Kritikakou, and S. He, "Energy-aware multiple mobile chargers coordination for wireless rechargeable sensor networks," *IEEE Internet of Things Journal*, vol. 6, no. 5, pp. 8202–8214, 2019.

[21] T. N. Nguyen, B.-H. Liu, S.-I. Chu, D.-T. Do, and T. D. Nguyen, "Wrsns: Toward an efficient scheduling for mobile chargers," *IEEE Sensors Journal*, vol. 20, no. 12, pp. 6753–6761, 2020.

[22] Z. Wei, M. Li, Q. Zhao, Z. Lyu, S. Zhu, and Z. Wei, "Multi-mc charging schedule algorithm with time windows in wireless rechargeable sensor networks," *IEEE Access*, vol. 7, pp. 156 217–156 227, 2019.

[23] M. Shin, J. Kim, and M. Levorato, "Auction-based charging scheduling with deep learning framework for multi-drone networks," *IEEE Transactions on Vehicular Technology*, vol. 68, no. 5, pp. 4235–4248, 2019.

[24] Y. Zhu, K. Chi, P. Hu, K. Mao, and Q. Shao, "Velocity control of multiple mobile chargers over moving trajectories in rf energy harvesting wireless sensor networks," *IEEE Transactions on Vehicular Technology*, vol. 67, no. 11, pp. 11 314–11 318, 2018.

[25] N. Gharaei, Y. D. Al-Otaibi, S. A. Butt, S. J. Malebary, S. Rahim, and G. Sahar, "Energy-efficient tour optimization of wireless mobile chargers for rechargeable sensor networks," *IEEE Systems Journal*, vol. 15, no. 1, pp. 27–36, 2021.

[26] T. M. Behera, S. K. Mohapatra, U. C. Samal, M. S. Khan, M. Daneshmand, and A. H. Gandomi, "I-sep: An improved routing protocol for heterogeneous wsn for iot-based environmental monitoring," *IEEE Internet of Things Journal*, vol. 7, no. 1, pp. 710–717, 2020.

[27] S. He, J. Chen, F. Jiang, D. K. Yau, G. Xing, and Y. Sun, "Energy provisioning in wireless rechargeable sensor networks," *IEEE Transactions on Mobile Computing*, vol. 12, no. 10, pp. 1931–1942, 2012.

[28] M. Choi, A. F. Molisch, and J. Kim, "Joint distributed link scheduling and power allocation for content delivery in wireless caching networks," *IEEE Transactions on Wireless Communications*, vol. 19, no. 12, pp. 7810–7824, 2020.

[29] L. Fu, P. Cheng, Y. Gu, J. Chen, and T. He, "Optimal charging in wireless rechargeable sensor networks," *IEEE Transactions on Vehicular Technology*, vol. 65, no. 1, pp. 278–291, 2016.

[30] B. Tong, G. Wang, W. Zhang, and C. Wang, "Node reclamation and replacement for long-lived sensor networks," *IEEE Transactions on Parallel and Distributed Systems*, vol. 22, no. 9, pp. 1550–1563, 2011.

[31] H. Dai, X. Wang, A. X. Liu, H. Ma, G. Chen, and W. Dou, "Wireless charger placement for directional charging," *IEEE/ACM Transactions on Networking*, vol. 26, no. 4, pp. 1865–1878, 2018.

[32] J. Matoušek, M. Sharir, and E. Welzl, "A subexponential bound for linear programming," *Algorithmica*, vol. 16, no. 4-5, pp. 498–516, 1996.

[33] E. Welzl, "Smallest enclosing disks (balls and ellipsoids)," *New Results and New Trends in Computer Science*, pp. 359–370, 1991.

[34] K. Helsgaun, "An effective implementation of the lin-kernighan traveling salesman heuristic," *European Journal of Operational Research*, vol. 126, pp. 106–130, 2000.

[35] F. Wang, J. Xu, and Z. Ding, "Multi-antenna noma for computation offloading in multiuser mobile edge computing systems," *IEEE Transactions on Communications*, vol. 67, no. 3, pp. 2450–2463, 2019.

[36] A. Boukerche, Q. Wu, and P. Sun, "A novel two-mode qos-aware mobile charger scheduling method for achieving sustainable wireless sensor networks," *IEEE Transactions on Sustainable Computing*, pp. 1–1, 2020.

[37] B. Dande, S.-Y. Chen, H.-C. Keh, S.-J. Yang, and D. S. Roy, "Coverage-aware recharging scheduling using mobile charger in wireless sensor networks," *IEEE Access*, vol. 9, pp. 87 318–87 331, 2021.

[38] G. Han, H. Wang, H. Guan, and M. Guizani, "A mobile charging algorithm based on multicharger cooperation in internet of things," *IEEE Internet of Things Journal*, vol. 8, no. 2, pp. 684–694, 2021.

Donghyun Lee received his B.S. degree in Computer Science and Engineering from Dongguk University, South Korea, in 2020. He is currently pursuing an M.S. degree in Computer Science and Engineering at Chung-Ang University, South Korea. His research interests include wireless networks, energy-efficient networks, multimedia communications, and the Internet of Things.

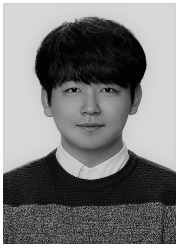

Cheol Lee received B.S. and M.S. degrees in Computer Science and Engineering from Chung-Ang University, South Korea, in 2018 and 2020. He is currently a technical engineer at NAVER Corporation, South Korea. His research interests include wireless networks, energy harvesting, and the Internet of Things.

Gunhee Jang received B.S. and M.S. degrees in Computer Science and Engineering from Chung-Ang University, South Korea, in 2019 and 2021, respectively. He is currently a Researcher with Qucell Networks, South Korea. His research interests include wireless networks, energy-efficient networks, 5G networks, and the Internet of Things.

Woongsoo Na received B.S., M.S., and Ph.D. degrees in Computer Science and Engineering from Chung-Ang University, Seoul, South Korea, in 2010, 2012, and 2017, respectively.

He is currently an Assistant Professor with the Department of Computer Science and Engineering, Kongju National University, Cheonan, South Korea. He was an Adjunct Professor at the School of Information Technology, Sungshin Womens University, Seoul, South Korea, from 2017 to 2018, and a Senior Researcher at the Electronics and Telecommunications Research Institute, Daejeon, South Korea, from 2018 to 2019. His current research interests include mobile edge computing, flying ad hoc networks, wireless mobile networks, and beyond 5G.

Sungrae Cho received his B.S. and M.S. degrees in electronics engineering from Korea University, Seoul, South Korea, in 1992 and 1994, respectively, and his Ph.D. degree in Electrical and Computer Engineering from the Georgia Institute of Technology, Atlanta, GA, USA, in 2002.

He is a Professor at the School of Computer Science and Engineering, Chung-Ang University (CAU), Seoul, South Korea. Prior to joining CAU, he was an Assistant Professor with the Department of Computer Sciences, Georgia Southern University, Statesboro, GA, USA, from 2003 to 2006, and a Senior Member of the Technical Staff at the Samsung Advanced Institute of Technology (SAIT), Kiheung, South Korea, in 2003. From 1994 to 1996, he was a Research Staff Member at the Electronics and Telecommunications Research Institute (ETRI), Daejeon, South Korea. From 2012 to 2013, he held a Visiting Professorship at the National Institute of Standards and Technology (NIST), Gaithersburg, MD, USA. His current research interests include wireless networking, ubiquitous computing, and ICT convergence. He has served numerous international conferences as an Organizing Committee Chair, such as *IEEE SECON*, *ICOIN*, *ICTC*, *ICUFN*, *TridentCom*, and *IEEE MASS*, as well as a Program Committee Member for conferences such as *IEEE ICC*, *MobiApps*, *SENSORNETS*, and *WINSYS*.

He has been a Subject Editor for *IET Electronics Letter* since 2018 and was an Editor for *Ad Hoc Networks Journal* (Elsevier) from 2012 to 2017.